Phases and phase transitions of (NaCl)1-x(NaCN)x

S. Elschner, K. Knorr, Alois Loidl

Angaben zur Veröffentlichung / Publication details:

Elschner, S., K. Knorr, and Alois Loidl. 1985. “Phases and phase transitions of (NaCl)1-x(NaCN)x.” *Zeitschrift für Physik B Condensed Matter* 61 (2): 209–15. https://doi.org/10.1007/bf01307778.

Phases and Phase Transitions of $(NaCl)_{1-x}(NaCN)_x$

S. Elschner
Fachbereich Physik der Universität des Saarlandes, Saarbrücken, Federal Republic of Germany

K. Knorr and A. Loidl
Institut für Physik der Universität Mainz, Federal Republic of Germany

$(NaCl)_{1-x}(NaCN)_x$ mixed crystals with CN-concentrations x of 0.87, 0.76, 0.71 and 0.65 have been investigated by X-ray powder diffraction. Apart from the cubic room temperature phase, a rhombohedral and an orthorhombic phase have been identified. In addition a glass state has been observed which is characterized by a strong broadening of the cubic powder lines. The phase diagram shows a wide coexistence gap between the non-cubic phases and the glass state.

I. Introduction

The alkali cyanides and the alkali cyanide-halide mixed crystals show a fascinating variety of structural phases. NaCN and KCN are cubic ($Fm3m$) at room temperature, centered orthorhombic ($Immm$) at intermediate and primitive orthorhombic ($Pmmn$) at low temperatures [1, 2]. $(KBr)_{1-x}(KCN)_x$ mixed crystals exhibit, besides the cubic high temperature phase, six non-cubic low temperature phases [3, 4]. Below a CN-concentration x of about 0.6 the compounds remain cubic down to lowest temperatures, but the diffraction patterns of X-ray and neutron experiments [4, 5] show a strong broadening of the Bragg reflections at lower temperatures. This new state is called glass state and is characterized by a frozen-in arrangements of statistical CN-orientations and lattice strains [6]. As for spin glasses the transition into the glass state is indicated by cusps of the susceptibility, in the present case of the dipolar and quadrupolar susceptibility [7].

A qualitative understanding of this complex structural behaviour can be obtained when one realizes that the CN-molecule is aspherical. Its orientational degrees of freedom are coupled to the translational i.e. phonon modes of the center of mass lattice. Hence the lattice deformations at the structural transitions are connected with changes of the orientational distribution. In NaCN for example, the CN-molecules of the cubic phase behave as almost free rotators with a slight preference for orientations along $\langle 100 \rangle$ [8]. In the orthorhombic phases the molecules are aligned along the former [110] direction with head-to-tail disorder in the upper and antiferroelectric order in the lower phase.

The decisive role of the orientational-translational coupling is also illustrated by the softening of the elastic shear constant c_{44} of the cubic phase [9]. The coupling can be translated into an effective CN $-$CN interaction of dipolar form [10]. The glass state is thought to be the consequence of the strong anisotropy of this interaction in combination with the chemical disorder of the halide-cyanide sublattice.

The various phases of the pure NaCl-type cyanides, KCN, NaCN, RbCN as a function of temperature and pressure can be arranged in a general phase diagram [11]. In this article we will investigate the phases and phase transitions of $(NaCl)_{1-x}(NaCN)_x$ as a function of x and T and will discuss the question if there is a general phase diagram for the mixed crystals.

II. Experimental Results and Analysis

Single crystals of $(NaCl)_{1-x}(NaCN)_x$ with $x=0.87$, 0.76, 0.71, 0.65 have been grown from the melt by J. Albers, University of Saarbrücken, and have been characterized by specific heat and dielectric experiments [12]. Their CN-concentrations have been determined from infrared and X-ray diffraction results.

Small slices of the original crystals have been used for the present study. The variation x of the CN-concentration across these small pieces is definitely less than 0.01.

The X-ray set up is identical to that of Ref. 4. Again, the raw diffraction data will be presented as counting rates versus channel number where the channel number is a roughly linear measure of the scattering angle 2θ. 25 channels correspond to about one degree in 2θ.

A) Phase Transitions

Three crystallographic phases, namely cubic, rhombohedral and orthorhombic, and a glass state can be identified in the powder patterns. The powder lines of the rhombohedral and of the orthorhombic phase can be all regarded as offsprings of the fcc lines. The results are illustrated by the Figs. 1–3 which show a section of the powder patterns centered at the position of the cubic (220)-line. The temperature dependence of the line positions is given in Fig. 4. The orthorhombic reflections are indexed in terms of a monoclinic cell containing four formula units with the cell parameters $a_m = c_m \mp b_m$, β_m. The results propose that the orthorhombic structure is identical to that of pure NaCN with the CN-molecules aligned along the former [110] direction.

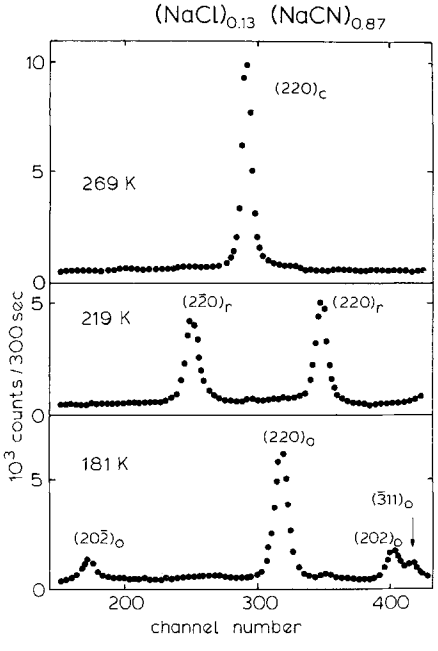

Fig. 1. Sections of powder patterns for $x=0.87$. The subscripts c, r, o refer to "cubic", "rhombohedral", "orthorhombic". The orthorhombic lines are indexed in terms of a monoclinic cell containing four formula units. 25 channels correspond to about one degree in the Bragg angle 2θ

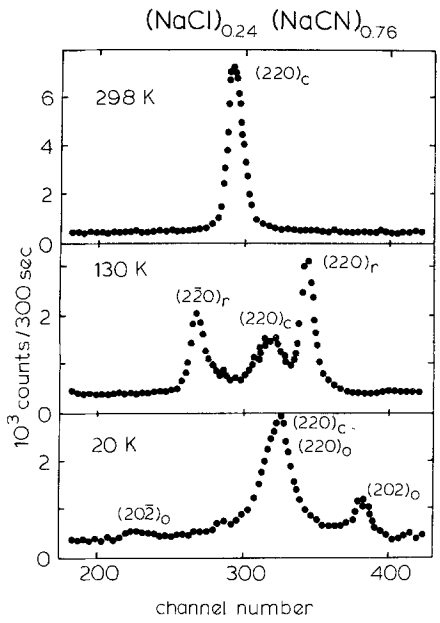

Fig. 2. Sections of powder patterns for $x=0.76$

A distinction of the electrically disordered and the antiferroelectric orthorhombic phase is not possible by X-ray diffraction. The space group of the rhombohedral phase with the cell parameters a_r and α_r is presumably $R\bar{3}m$. The cell parameters are listed in Table 1.

The sample with the highest CN-concentration, $x=0.87$, shows wide temperature ranges where the three crystallographic structures – cubic, rhombohedral and orthorhombic – exist in pure form. These single phase regions are separated by narrow coexistence regions cubic-rhombohedral and rhombohedral-orthorhombic which are about 10 K wide (Fig. 4). The transition temperatures T_{c1} and T_{c2}, as defined by the midpoints of the coexistence regions, are 241 K and 204 K. Clearly the transitions are discontinuous. Both phase transitions are confirmed by measurements of the specific heat and of the real part of the dielectric constant [12].

The sample with $x=0.76$ shows a more complex diffraction pattern. At a temperature T_{c1} of 195 K, below the cubic single phase region, the sample enters a cubic-rhombohedral coexistence range. The percentage of the cubic component decreases from about 50% just below T_{c1} to about 30% at the second transition temperature T_{c2} of 92 K where the rhombohedral lines disappear in favour of orthorhombic ones with no apparent change of the cubic intensities. The coexistent cubic and orthorhombic lines are considerably broadened (Fig. 2), presumably because of distributions of the cell parameters. The onset of the low temperature

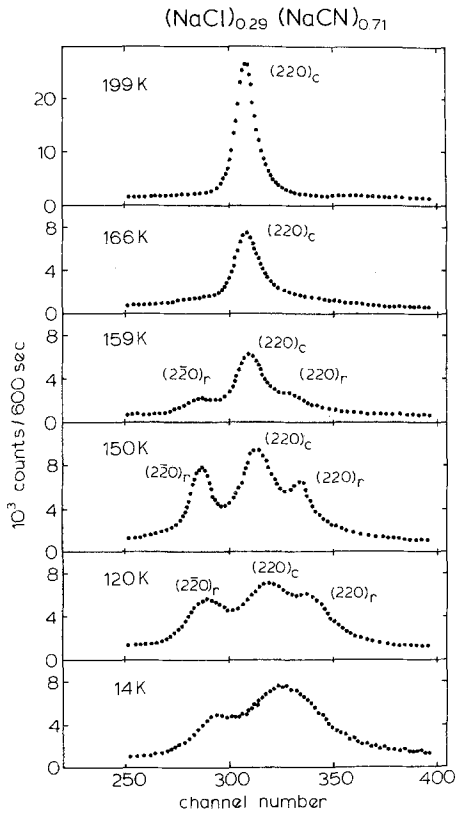

Fig. 3. Sections of powder patterns for $x=0.71$

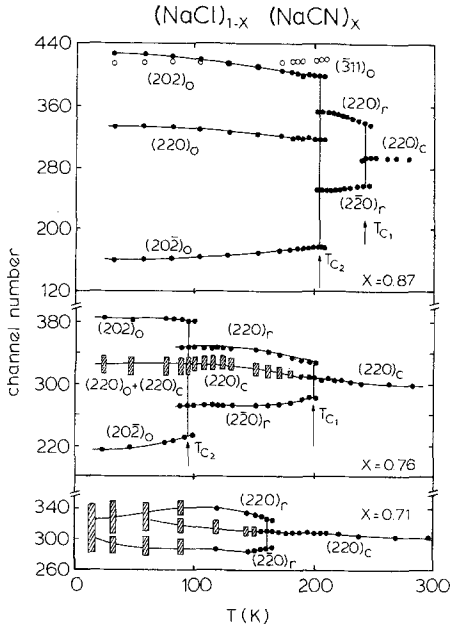

Fig. 4. The splitting of the $(220)_c$ cubic powder line as a function of temperature in the three ordering mixed crystals

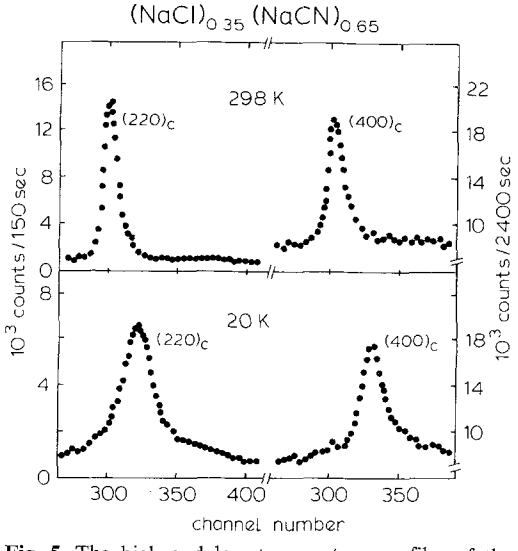

Fig. 5. The high and low temperature profiles of the $(220)_c$ and the $(400)_c$ powder line for $x=0.65$

phases at T_{c1} and T_{c2} is again discontinuous. Below 240 K, in particular at temperatures close to the phase transitions, weak extra powder lines have been observed which could not be assigned to any of the three phases.

In the third sample, $x=0.71$, the Bragg peaks of the cubic phase attain wings of diffuse intensity, growing with decreasing temperature. First indications of this behaviour could already be found for $x=0.76$. At about 160 K rhombohedral lines develop out of these broad cubic patterns (Fig. 3). From about 150 K down to about 90 K relatively sharp rhombohedral lines coexist with broad cubic diffraction

Table 1. Cell parameters of $(NaCl)_{1-x}(NaCN)_x$

x	T(K)	Structure	Cell parameters (A resp. deg.)	Cell volume (A^3)
0.87	268	cubic	$a_c=5.86$	201.2
	228	rhomb	$a_r=5.85$ $\alpha_r=85.2$	200.5
	22	orth	$a_0=6.00$ $b_0=5.50$ $\beta_0=104.0$	192.1
0.76	290	cubic	$a_c=5.83$	198.2
	121	(cub)+rhomb	$a_r=5.79$ $\alpha_r=86.0$	193.6
	20	(cub)+orth	$a_0=5.75$ $b_0=5.63$ $\beta_0=97.8$	189.6
0.71	290	cubic	$a_c=5.81$	196.1
	139	(cub)+rhomb	$a_r=5.76$ $\alpha_r=87.5$	190.6
0.65	290	cubic	$a_c=5.79$	194.1

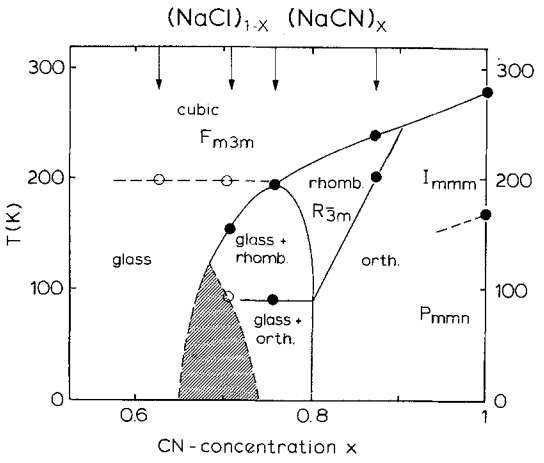

Fig. 6. The tentative x, T-phase diagram. The arrows indicate the CN-concentrations studied in the present work. Solid points give experimentally established transition temperatures between crystallographic phases. The data on pure NaCN are taken from Ref. 1. Open symbols indicate the onset of line broadening. Two interpretations are possible for the hatched x, T-range: re-entrant glass behaviour or a coexistence between the quasicubic glass state and heavily strained remainders of the non-cubic phases

maxima. Below 90 K these two components merge in broad distributions which can no longer be clearly assigned to crystallographic structures, but which are nevertheless centered at the Bragg positions of a fcc-lattice (Fig. 3). We conclude that there is a coexistence of a quasicubic structure with broadened lines, the glass state, and the rhombohedral phase. The fraction of the two components is about 60:40. Below 90 K the rhombohedral splitting decreases again, while the line widths increase further. We will comment on this point later.

The sample with $x=0.65$ remains cubic down to lowest temperatures, the width of the cubic lines increases with decreasing temperature (Fig. 5). The broadening occurs in T_{2g} scattering geometry as can be derived from the different line widths of the Bragg reflections. For example Fig. 5 shows that the (400) line is narrower than the (220) line in spite of the higher scattering angle. In analogy to $(KBr)_{1-x}(KCN)_x$ we attribute these quasicubic patterns to the glass state.

A schematic x, T-phase diagram of $(NaCl)_{1-x}(NaCN)_x$ is proposed in Fig. 6, where the full points indicate transitions between crystallographic phases. The open points give the temperature where the line broadening effects become visible.

B) Order Parameters

As the rhombohedral and the orthorhombic structure can be regarded as homogeneous deformations of the cubic structure, the transitions cubic to rhombohedral and cubic to orthorhombic are Landau type, ferroelastic phase transitions [13], whereas the rhombohedral to orthorhombic transition is martensitic in the sense that there is no group-subgroup relation between the two phases. The spontaneous strains of the rhombohedral and the orthorhombic phase relative to the cubic one are the appropriate order parameters. For $x=0.87$ Fig. 8 shows that the cell volume V is not affected by the cubic to rhombohedral transition. The rhombohedral phase is thus characterized exclusively by the three component shear order parameter $\Delta\alpha=\Delta\beta=\Delta\gamma=90°-\alpha_r$. $\Delta\alpha(T)$ is shown in Fig. 7. The order parameter and its jump at T_{c1} decreases with decreasing CN-concentration.

The spontaneous deformation tensor of the orthorhombic phase contains contributions of all three cubic symmetry strains (A_{1g}, T_{2g}, E_g), here written as the volume change ΔV, the one component shear $\Delta\beta=\beta_m-90°$, $\Delta\alpha=\Delta\gamma=0$ and the uniaxial compression b_m/a_m-1. The temperature of these quantities is depicted in Fig. 8. Following the symmetry considerations of Ref. 13, the primary order parameter is $\Delta\beta$. The orthorhombic order parameters for $x=0.76$ are hard to determine from the diffraction data. For $x=0.76$ they are roughly 2/3 of those for $x=0.87$. The peculiar shapes of the orthorhombic lines for $x=0.76$ - see e.g. the sharp (202) and the broad $(20\bar{2})$ of Fig. 3 - can be explained by assuming distributions of the order parameter with the constraint that its components are proportional to each other. The order parameter of orthorhombic NaCN [14] is

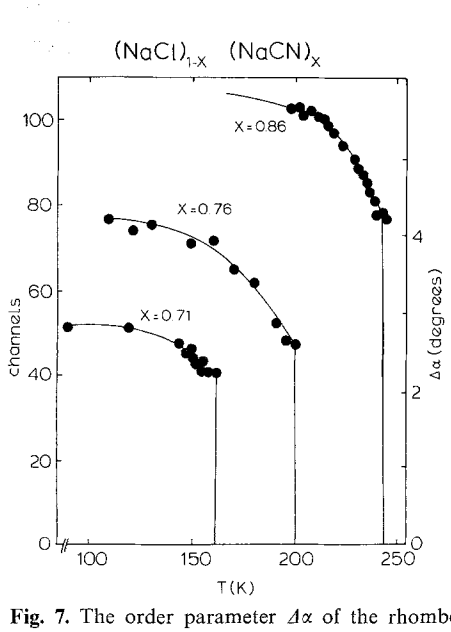

Fig. 7. The order parameter $\Delta\alpha$ of the rhombohedral phase, $\Delta\alpha=90°-\alpha_r$ where α_r is the rhombohedral cell angle

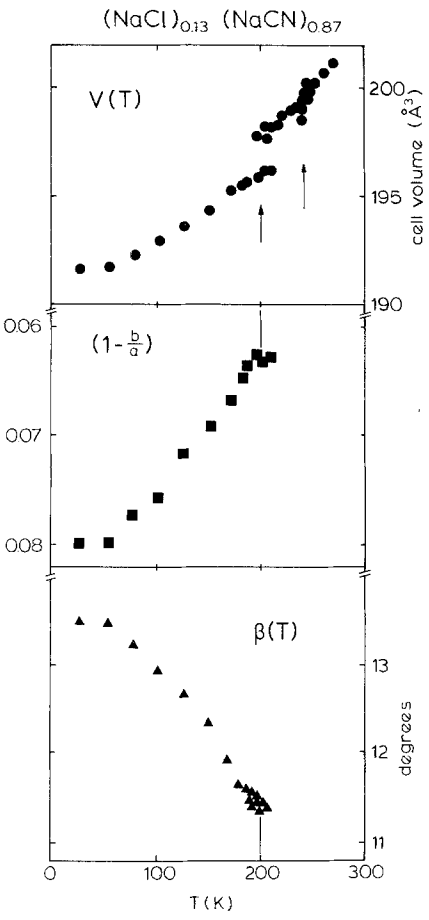

Fig. 8. Quantities characterizing the elementary cell for $x=0.87$. The arrows indicate the two transition temperatures cubic to rhombohedral and rhombohedral to orthorhombic. In the orthorhombic phase the cell volume V the angle β and the quantity $1-b/a$ refer to a monoclinic cell with the parameters $a=c$, b, β. $1-b/a$, β and the volume change are the ferroelastic order parameters of the orthorhombic phase

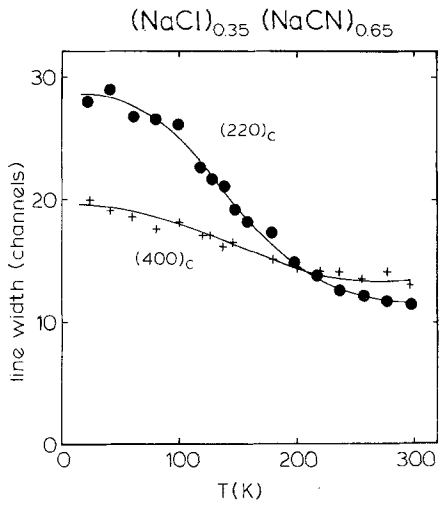

Fig. 9. The temperature dependence of the $(220)_c$ and $(400)_c$ line widths for $x=0.65$

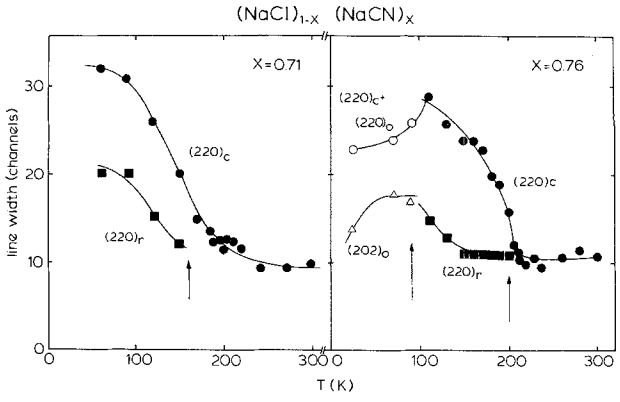

Fig. 10. The temperature dependence of the width of the $(220)_c$ cubic line and its offsprings in the non-cubic phases for $x=0.76$ and 0.71

eleven percent higher that that of the mixed crystal with $x=0.87$.

C) The Glass State

The sample with $x=0.65$ remains cubic down to the lowest temperatures with a strong broadening of the diffraction lines at lower temperatures. Recently it has been demonstrated for $(KBr)_{1-x}(KCN)_x$ that the temperature where this extra breadth of the Bragg lines becomes apparent can be identified as the freezing temperature T_F [4, 5]. It is the same temperature where the sound velocity exhibits a minimum [5, 6] and where in an inelastic neutron experiment a narrow central line appears in the scattered intensities [6]. The line broadening becomes detectable below 200 K. The (220) line exhibits an increase of the width which is much stronger than for the (400) line (Fig. 9), a clear demonstration that the dominant broadening is of T_{2g} symmetry, as in the KBr-based mixed crystals.

Recent ^{23}Na NMR experiments [15] for samples with the same concentration $x=0.65$ also give evidence for a freezing of lattice strains below 200 K. The coupling of the ^{23}Na nuclear quadrupole moments with the electric field gradient (EFG) shifts the nuclear Zeeman levels and thus renders possible a determination of the EFGs at the Na-sites.

In contrast to a perfect cubic lattice where the EFGs vanish as a consequence of symmetry in a mixed system the local environments in general deviate from cubic symmetry and one therefore obtains a distribution of ^{23}Na resonance frequencies. It could be ascribed to a gaussian distribution of the EFGs, the width of which measures the mean deviation

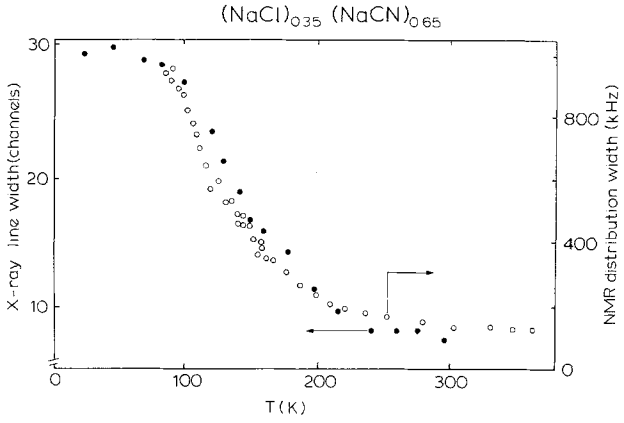

Fig. 11. Temperature dependences of the $(220)_c$ line width and of the electric field gradient distribution width at the ^{23}Na-sites [15] for $x=0.65$

from local cubic symmetry. In exactly the same temperature region where the broadening of the Bragg-peaks is observed also the width of the EFG distribution increases (Fig. 11). The effect is very drastic and nearly covers one order of magnitude. It should be stressed out, that the time scales of the X-ray and NMR experiments are considerably different. The X-ray experiments provide a snapshot of the atomic arrangement whereas the NMR experiments average over a time scale of at least 1 μsec. This is long compared to the correlation times of the molecular motions [15, 16]. Thus the freezing of the lattice strains observed with both methods is rather static than dynamic.

The samples with $x=0.71$ and 0.76 show a behaviour unknown in $(KBr)_{1-x}(KCN)_x$. As mentioned above, the cubic phases coexist with non-cubic ones. Figure 10 shows the widths of the coexistent lines. Below 200 K the cubic lines show the monotonic increase with decreasing temperature, known from the $x=0.65$ sample where the non-cubic phases are absent. Hence, we conclude that for these CN-concentrations the glass state develops in coexistence with non-cubic components.

Are the non-cubic components crystalline or glass-like? Guided by the line widths of Fig. 10 we suggest: for $x=0.76$ and $150\,K<T<200\,K$ the rhombohedral component is crystalline, as the rhombohedral powder lines are sharp. For $90\,K<T<150\,K$ the rhombohedral lines are broadened. We leave it to the reader if he is willing to accept the idea of a quasirhombohedral glass state coexistent with the quasicubic component. Below 90 K the rhombohedral component orders orthorhombically, the line widths decrease again with decreasing temperature, though they always exceed the instrumental resolution (of about 10 channels).

For $x=0.71$ the rhombohedral lines appear at about 160 K, their widths increase with decreasing temperature - again one might think of the evolution of a quasirhombohedral glass state. At about 90 K there are qualitative changes of the diffraction pattern (Fig. 3) which hamper a quantitative analysis in terms of crystallographic structures. We propose two possible interpretations: *i)* there is an attempted, presumably orthorhombic ordering of the rhombohedral components analogous to $x=0.76$, or *ii)* one abandons the idea of coexisting components at all and thinks of a unique glass state. The two possibilities are indicated in the phase diagram. It is important to note that case *ii)* leads to a reentrant-type of transition.

We are aware that we use the term "glass" in a somewhat superficial and purely heuristic meaning, namely for a state with broadened powder lines, but that is the amount of information which one can obtain from an X-ray study. A characterization of the non-cubic glass states by complementary methods like e.g. ultrasonic measurements which have been helpful for $(KBr)_{1-x}(KCN)_x$ would be seriously handicapped by the multidomainstructures of the present non-cubic phases.

III. Discussion

Starting from the cubic phase a spontaneously sheared low temperature phase of the pure cyanide and a frustrated state at low temperatures and low CN-concentrations are quite plausible consequences of the bilinear coupling between the CN-orientations and the strains of the center of mass lattice. But that is about how far our theoretical understanding goes in the moment. Already the orientational distributions with ⟨111⟩ maxima for KCN and ⟨100⟩ maxima for NaCN and the cubic to orthorhombic phase transitions of these compounds is not yet theoretically explaind [8], not to mention the various phases of the mixed crystals. In this situation we want to point out a surprising aspect of the rhombohedral phase. Assuming ⟨111⟩ easy directions in the cubic phase, a cubic-rhombohedral transition with a stretching of the cell along [111] connected with a [111] easy direction appears to be the most obvious choice of a ferroelastic phase transition in the cyanide systems with a soft elastic shear constant c_{44}. This transition occurs in fact in CsCl-type CsCN [17], but not in the NaCl-type cyanides. Here one finds instead: *i)* a stretched rhombohedral cell in combination with [100], [010], [001] easy directions in $(NaCl)_{1-x}(NaCN)_x$, *ii)* a cell squeezed along [111] and $[\bar{1}11]$, $[1\bar{1}1]$, $[11\bar{1}]$ easy directions

in $(KBr)_{1-x}(KCN)_x$, here we have assumed that the easy directions of the rhombohedral phase evolve from the easy directions of the cubic phase of the corresponding pure cyanide. It is easily seen that *i)* and *ii)* require rapid reorientations of the CN-molecule. A static alignment of the $4 \cdot x$ CN-molecules along three easy directions would be incompatible with the rhombohedral symmetry. Thus *i)* and *ii)* cannot be low temperature states and seem to be "dead ends" from which the systems can escape by drastic changes of the structure only. These elementary consideration illustrate the problem of the cyanide structures.

The results on the two series of mixed crystals support the view that the onset of the glass state for $x < x_g$ is connected with a reduction of the first order character of the transition from the cubic to the elastically ordered phase when approaching x_g from higher CN-concentrations, i.e. the glass state is announced by a softening of the elastic constant c_{44} and a concomitant growth of diffuse scattering around the Bragg reflections in a X-ray experiment.

IV. Summary

Comparing $(NaCl)_{1-x}(NaCN)_x$ and $(KBr)_{1-x}(KCN)_x$ we note a general analogy as there are three principal regions in the x, T-phase diagram: the cubic phase at high T, the non-cubic crystalline phases at low T and high x and the glass state at low x and T. The cubic-non-cubic transition temperatures $T_c(x)$ and the order parameters decrease with decreasing x. All non-cubic phases have strong shear components.

The NaCl-based mixed crystals differ from the KBr-based mixed crystals in the following points:

i) there is a wide coexistence gap between the non-cubic phases and the glass state

ii) the rhombohedral phase has a wider existence region and is stretched rather than squeezed

iii) the phase below the rhombohedral one is the orthorhombic structure of the pure cyanide rather than a new monoclinic structure.

We are grateful to J. Albers and A. Klöpperpieper for providing the samples and to J. Petersson for stimulating discussions.
This work was supported by the Sonderforschungsbereich 130 "Ferroelektrika", Saarbrücken.

References

1. Verweel, H.J., Bijvoet, J.M.: Z. Kristallogr. Mineral. **100**, 201 (1941)
2. Fontaine, D.: C.R. Acad. Sci Ser. B**281**, 443 (1975)
3. Rowe, J.M., Rush, J.J., Susman, S.: Phys. Rev. B**28**, 3506 (1983)
4. Knorr, K., Loidl, A.: Phys. Rev. B**31**, 5387 (1985)
5. Loidl, A., Müllner, M., McIntyre, G., Knorr, K., Jex, H.: Solid State Commun. **54**, 367 (1985)
6. Michel, K.H., Rowe, J.M.: Phys. Rev. B**22**, 1417 (1980)
7. Loidl, A., Feile, R., Knorr, K.: Phys. Rev. Lett. **48**, 1263 (1982)
8. Rowe, J.M., Hinks, D.G., Prince, D.L., Susman, S., Rush, J.J.: J. Chem. Phys. **58**, 2039 (1973)
9. Haussühl, S., Eckstein, J., Recker, K., Wallrafen, F.: Acta Crystallogr. Sect. A**33**, 847 (1977)
10. Michel, K.H., Naudts, J.: Phys. Rev. Lett. **39**, 212 (1977)
11. Dultz, W., Krause, H.: Phys. Rev. B**18**, 394 (1978)
12. Albers, J., Klöpperpieper, A., Müser, H.: (to be published)
13. Parlinski, K.: Z. Phys. B - Condensed Matter **56**, 51 (1984)
14. Yamamoto, S., Shinnaka, Y.: J. Phys. Soc. Jpn. **50**, 1417 (1981)
15. Elschner, S., Petersson, J.: (to be published); Elschner, S.: Proc. XXIInd Congress Ampere. K.A. Müller, R. Kind, J. Roos (eds.), p. 86. Zürich 1984
16. Albers, J., Elschner, S., Klöpperpieper, A., Petersson, J.: Ferroelectrics **55**, 101 (1983)
17. Knopp, G., Knorr, K., Loidl, A., Haussühl, S.: Z. Phys B - Condensed Matter **51**, 259 (1983)

S. Elschner
Fachbereich Physik
Universität des Saarlandes
D-6600 Saarbrücken
Federal Republic of Germany

K. Knorr
A. Loidl
Institut für Physik
Universität Mainz
Staudinger Weg 7
D-6500 Mainz
Federal Republic of Germany